

## CHAPTER 13

### SIMULATION OF PROPAGATING NONLINEAR WAVE GROUPS

Paul de Haas<sup>1, 2</sup>, Maarten Dingemans<sup>1</sup> and Gert Klopman<sup>1</sup>

#### Abstract

Propagating nonlinear waves can be computed with a time-domain numerical method based on a boundary element method. For the simulation of propagating wave groups a domain decomposition method is used to increase the efficiency of the model and to enable simulation over many wave periods. In the computations described in this paper several nonlinear formulations for an initial wave group signal are used to investigate their ability to describe a wave group of fixed form. A difficulty consists of the imposition of the boundary conditions at the unknown free-surface elevation. The nonlinear contributions to the first-order signal are related to the generation of free waves as computed by the model.

#### 1 Introduction

Long-wave motion is usually split up between a bound part which is due to nonlinear difference interactions between short sea and swell waves and a free part which are waves that move with their own celerity according to an appropriate dispersion relation. It is known that when waves travel over an uneven bottom, energy in the bound component of the long waves is transformed to the free components.

In this paper we present a two-dimensional (2DV) time-domain numerical method, based on a boundary element method, which computes the propagation of waves with the exact nonlinear boundary conditions over an arbitrary bottom geometry. It is therefore able to simulate the generation of free long waves due to an uneven bottom. A model problem used by Dingemans et al. [3], is used as reference for the computations presented here. Different formulations of the nonlinear wavegroup signal are tested for their suitability to describe a wave group of fixed form over a horizontal bottom. Such a signal can then be used

---

<sup>1</sup>Delft Hydraulics, P.O. Box 177, 2600 MH Delft, The Netherlands

<sup>2</sup>University of Twente, Faculty of Applied Mathematics, P.O. Box 217, 7500 AE Enschede, The Netherlands

as an initial signal for problems with a bottom topography in order to study the generation of free long-wave components.

Because the study of such problems requires large computational effort, the use of efficient numerical techniques is imperative. Here we will present a domain decomposition method which reduces the computational costs of the boundary element method considerably.

This paper is organized as follows. First the numerical method is described in Section 2. In Section 3 the domain decomposition method is described and its efficiency is discussed. In Section 4 some nonlinear formulations of a wave group signal are discussed and used as initial signal for the computations. Finally some conclusions will be stated in Section 5.

## 2 Numerical method

In the mathematical model for nonlinear water waves considered here, the motion of the water is described by the usual potential-flow equations for inviscid irrotational fluid motion with a free surface on water of varying depth. It is described by the field equation for the velocity potential  $\phi$  (Laplace's equation)

$$\Delta\phi = 0, \quad (1)$$

and the boundary conditions on the free surface  $\partial\Omega_{FS}$

$$\left. \begin{aligned} \frac{D\phi}{Dt} &= \frac{1}{2}(\nabla\phi)^2 - gz - \frac{p}{\rho} \\ \frac{D\mathbf{x}}{Dt} \cdot \mathbf{n} &= \frac{\partial\phi}{\partial n} \end{aligned} \right\} \mathbf{x} \in \partial\Omega_{FS} \quad (2)$$

and on the bottom  $\partial\Omega_B$

$$\frac{\partial\phi}{\partial n} = 0, \quad \mathbf{x} \in \partial\Omega_B. \quad (3)$$

Appropriate in- and outflow boundary conditions are formulated on the lateral boundaries.

The numerical method consists of a time marching scheme for the evolution of the free surface and its boundary conditions. At every time-step, Laplace's equation for the velocity potential has to be solved. This is done with a boundary element method (BEM). In the BEM, Laplace's equation is solved by writing it as a set of integral equations over the boundary (one equation for every node). These integral equations are first discretized. Then, by using the boundary conditions a system of linear equations is built and subsequently solved. Insertion into equations (2) of the solution obtained in this way, provides the time derivatives which are needed for the time marching scheme.

Boundary element methods are very suitable for solving Laplace's equation on such domains because they only require a discretization of the boundary of the domain. Compared with field discretization methods, the advantages of a BEM are a much smaller amount of grid points and a natural description of the evolution of the free surface. See [1] for a description of a three-dimensional

method. The computations described here were performed with a code developed for two-dimensional simulations based on the work of these authors.

For the computation of large-scale wave problems the solution algorithm for Laplace's equation is the bottleneck. It involves both the discretization of the boundary integral equations and the solution of the resulting system of linear equations. The time marching scheme requires a minor part of the total CPU-time. Furthermore, memory requirements for solving Laplace's equation depend quadratically on the number of grid points. These problems can be reduced considerably by the use of a domain decomposition method.

### 3 Domain decomposition

#### 3.1 Description

The domain decomposition method described here consists of a division of the computational domain into subdomains (see Figure 1) and an iterative procedure which generates a sequence of solutions on the subdomains that converges towards the solution on the original domain.

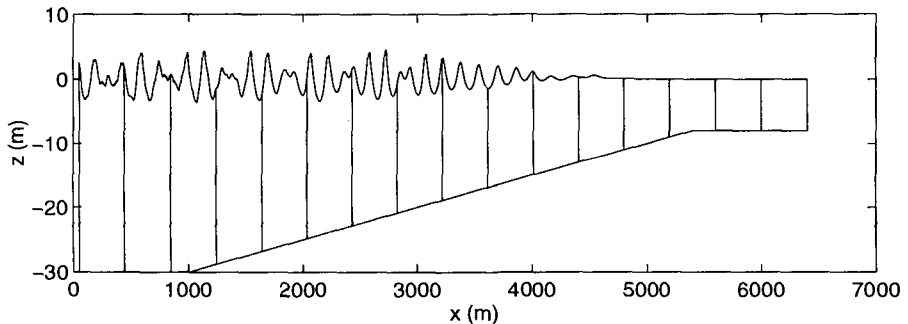


Figure 1: Decomposed domain

Every step of the iterative procedure consists of first solving Laplace's equation for the potential  $\phi$  on the separate subdomains simultaneously and secondly formulating new boundary conditions on the subdomain interfaces. In the latter part the subdomain problems are coupled.

There are many possibilities in the way information can be exchanged between the subdomains. We have chosen here to use the so-called DD/NN-scheme. Every odd step of the iterative procedure Dirichlet conditions are imposed on all interfaces. Neumann conditions are imposed at all even steps. These steps are illustrated in Figure 2 for the first two steps of a two-subdomain problem.

This scheme is also known as a Neumann-Neumann preconditioner in the context of domain decomposition methods for field discretization techniques. See e.g. [4]. In the field of time-domain BEM's a similar technique was used by Wang

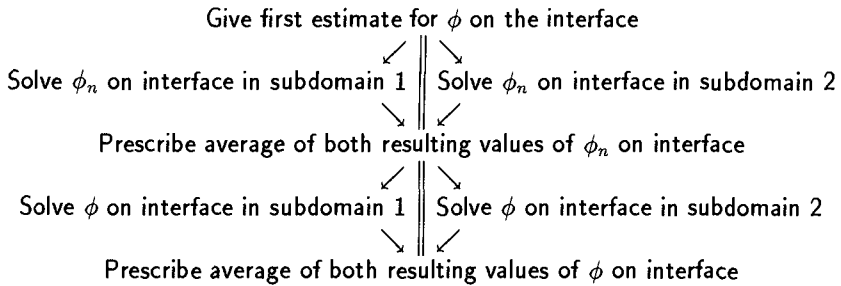


Figure 2: Schematic representation of the DD/NN-scheme

et al. [8]. In their work interfaces are used to formulate a block-structured matrix which is then solved iteratively. For a general impression of work being done in the field of domain decomposition the reader can consult [7].

### 3.2 Convergence characteristics

The performance of the domain decomposition method is determined here by the convergence of the iterative process. The convergence of the process can be judged by considering the jump across the interface between the solutions on both sides of each interface. The convergence on different interfaces depends on the geometrical form of the subdomains. This aspect has been subject of previous investigations [2] and the main conclusions given there are:

- The convergence of the iterative procedure deteriorates as the length-to-height ratio of the subdomains decreases and if there is more asymmetry near the interfaces due to a disturbed free surface or an uneven bottom.
- Therefore, given a fixed length of the computational domain, the convergence of the iterative procedure deteriorates as the number of subdomains  $N$  increases.
- Given a fixed length-to-height ratio of the subdomains, the convergence rate does not change as the number of subdomains increases, in the case of rectangular subdomains of equal size. In applications with a disturbed free surface we have seen that convergence is determined by the interface with the worst convergence. The number of iterations has an upper bound which is independent of  $N$ .

### 3.3 Efficiency

The efficiency of the domain decomposition technique is of course related to the convergence of the iterative method. It can be considered for the two cases mentioned above.

- If for a computational domain with a fixed length the number of subdomains is increased, on the one hand the number of required iterations will increase. On the other hand, the CPU-time to solve Laplace's equation per subdomain decreases, since the subdomains becomes smaller. It appears that there is a certain optimal number of subdomains (with respect to CPU-time) to solve a given water-wave problem. See [2].
- If subdomains are used with a fixed length-to-height ratio, the number of iterations and therefore the computational costs per subdomain, have an upper bound independent of the number of subdomains. This implies that the computational cost per time step depend at most linearly on the size of the computational domain.

In the application of the domain decomposition technique to the time-domain numerical method described here, it is possible to subdivide the domain differently every time step, adjusted to the presence of a wave signal. We have chosen to use a fixed initial subdivision of the computational domain with subdomains of equal size so that no reorganization of data over the subdomains is necessary and the number of grid points in all subdomains is the same.

## 4 Simulation of some nonlinear wave group signals

### 4.1 Introduction

In Liu and Dingemans [5] and Dingemans et al. [3] a mathematical model is described for the wave envelope  $A$  of a carrier wave signal. In this model third-order equations are derived with a multiple-scales technique for a first-order carrier wave signal given in complex notation by

$$\eta_1(x, t) = \frac{1}{2}(Ae^{i\chi_0} + *) \quad (4)$$

and

$$\phi_1(x, z, t) = \frac{1}{2} \left( -\frac{g \cosh(k_0(z+h))}{\omega \cosh(k_0 h)} i A e^{i\chi_0} + * \right) \quad (5)$$

with  $\chi_0 = k_0 x - \omega_0 t$ , being the phase function of the carrier wave. The  $*$ -symbol denotes the complex conjugate of the preceding term.

From solvability conditions of the third order equations, evolution equations are derived for the envelope  $A$ . For a horizontal bottom these equations simplify to a nonlinear Schrödinger (NLS) equation. See also Mei [6]. This equation admits several steady solutions for  $A$  which can be used to create an initial signal for a simulation.

In our computations we have chosen a soliton-solution described by the envelope function  $A$  as:

$$A(x, t) = a \operatorname{sech} \left( \sqrt{\frac{-\nu_1}{\partial C_g / \partial k_0}} a \cdot (x - C_g t) \right) \exp \left\{ -i \frac{\nu_1 a^2}{2} t \right\} \quad (6)$$

in which  $a$  and  $C_g$  are the amplitude and the group velocity of the carrier wave.  $\nu_1$  is a long expression in terms of characteristic quantities of the carrier wave and is given in Dingemans et al. [3], p. 364. The parameters have been evaluated for  $a = 1$  m,  $\omega_0 = 2\pi/6$  rad/s and  $h = 12$  m. The corresponding wave length  $L_0$  and group velocity  $C_g$  according to linear theory are equal to 50.73 m and 5.52 m/s respectively. Based on an elevation  $1 \cdot 10^{-3}$  times the maximum elevation, the wave group has a length of approximately 1850 m.

In the computations a known elevation  $\eta(x, t)$  is required as the initial disturbance of the free surface. The panel method furthermore requires an initial value of the potential  $\phi$  on the free surface which imposes the initial velocity field on the free surface. In the third-order model it is, just as  $\eta$ , given in terms of the third-order perturbation serie. Because of the large and complex expressions associated with the series, we have tried a number of alternatives and have studied the degree in which they describe a signal that propagates undisturbed over a horizontal bottom. These alternatives will be described next.

#### 4.2 Formulations for free-surface elevation and potential

A difficulty of simulating nonlinear wave signals consists of the imposition of the boundary conditions at the unknown free-surface elevation. In perturbations techniques, one usually expands free-surface elevation and potential around the still-water level  $z = 0$  and the potential is evaluated at the still-water level. In the numerical approach, the grid points are located at  $z = \eta$  so that evaluations there deviate from those of the perturbation approach. A Taylor expansion for  $\phi$  can be used to account for the location of the free surface at  $z = \eta$ :

$$\phi(x, z, t)|_{z=\eta} = \phi(x, 0, t) + \eta(x, t) \frac{\partial \phi}{\partial z}(x, 0, t) + O(\eta^2). \quad (7)$$

Besides the first order expressions given in equations (4) and (5) we have used a Stokes' second-order contribution given by

$$\eta_2(x, t) = \frac{1}{2} \left( \frac{1}{4} \frac{k_0 \cosh(k_0 h)}{\sinh^3(k_0 h)} [2 + \cosh(2k_0 h)] A^2 e^{2ix_0} + * \right) \quad (8)$$

and

$$\phi_2(x, z, t) = \frac{1}{2} \left( \frac{3\omega \cosh(2k_0(z+h))}{8 \sinh^4(k_0 h)} i A^2 e^{2ix_0} + * \right). \quad (9)$$

and a bound long-wave contribution based on the linearized depth-integrated mean-flow equations. See [3]. The free-surface elevation  $\zeta$  and potential  $\phi_{bl}$  of this wave are given by

$$\zeta(x, t) = \frac{2c_g/c - \frac{1}{2}}{2(c_g^2 - gh)} g \left( |A(-c_g t)|^2 - \langle |A|^2 \rangle \right) \quad (10)$$

and

$$\phi_{bl}(x, t) = \int_{-\infty}^x \frac{\partial \phi}{\partial x'} dx' = \int_{-\infty}^x u dx' = \int_{-\infty}^x \frac{c_g}{h} \zeta dx' \quad (11)$$

$$= \frac{2c_g/c - \frac{1}{2} c_g g}{2(c_g^2 - gh)} \frac{c_g g}{h} \int_{-\infty}^x (|A|^2 - \langle |A|^2 \rangle) dx'. \quad (12)$$

$\langle |A|^2 \rangle$  denotes the mean value of  $|A|^2$  over a time interval much longer than the wave group period. For the soliton solution (6),  $\langle |A|^2 \rangle = 0$ .

### 4.3 Results

For our computations we have selected a number of formulations which are tabulated in Table 1. These initial signals were used in simulations over 60 wave

Table 1: Initial signal for the various computations

	$\eta$	$\phi$	using formula (7)
run 1	$\eta_1$	$\phi_1$	no, $\phi$ evaluated at $z = \eta$
run 2	$\eta_1$	$\phi_1$	no, $\phi$ evaluated at $z = 0$
run 3	$\eta_1$	$\phi_1$	yes
run 4	$\eta_1 + \eta_2$	$\phi_1 + \phi_2$	no, $\phi$ evaluated at $z = 0$
run 5	$\eta_1 + \zeta$	$\phi_1 + \phi_{bl}$	no, $\phi$ evaluated at $z = 0$
run 6	$\eta_1 + \eta_2 + \zeta$	$\phi_1 + \phi_2 + \phi_{bl}$	no, $\phi$ evaluated at $z = 0$

periods in a computational domain with length 5000 m. Free-surface collocation points were distributed over  $z = \eta(x)$  with equal horizontal distances. The resolution of the computational configuration was taken the same for all simulations and is given by  $\Delta x = 2.5 \text{ m} \approx L_0/20 \text{ m}$  on the free surface and  $\Delta t = T_0/20 \text{ s}$ .

The results are illustrated best by showing the free-surface elevation at  $t = 45T$  for the different computations. Run 1 has been shown separately in a larger plot in order to show the details better. The result of run 3 is similar to that of run 1, because the vertical profile of  $\phi_1$  is almost linear in the range  $-\eta \leq z \leq \eta$  and differences between the evaluation of  $\phi_1$  at  $z = \eta$  (run 1) and the use of equation (7) (run 3) are hardly discernible. Therefore results of run 3 are not shown here.

A typical feature common to all computations is the generation of small left-going signals. In Figure 3 wave groups with carrier waves with a wave period of approximately 6.0 s (around  $x = 200 \text{ m}$ ) and 3.8 s (around  $x = 700 \text{ m}$ ) can be seen. Their group velocities are equal to 4.4 and 3.1 m/s respectively. Not visible in Figures 3 and 4 is a small left-going *long* wave ( $c = 11.1 \text{ m/s}$ ) which at this point of the computation has already left the computational domain. The left-going signal is the smallest in runs 2 and 5.

There is also a right-going free-long wave (around  $x = 4400 \text{ m}$ ) in all computations. The computed phase velocity of this wave equals 11.1 m/s where as  $\sqrt{gh}$

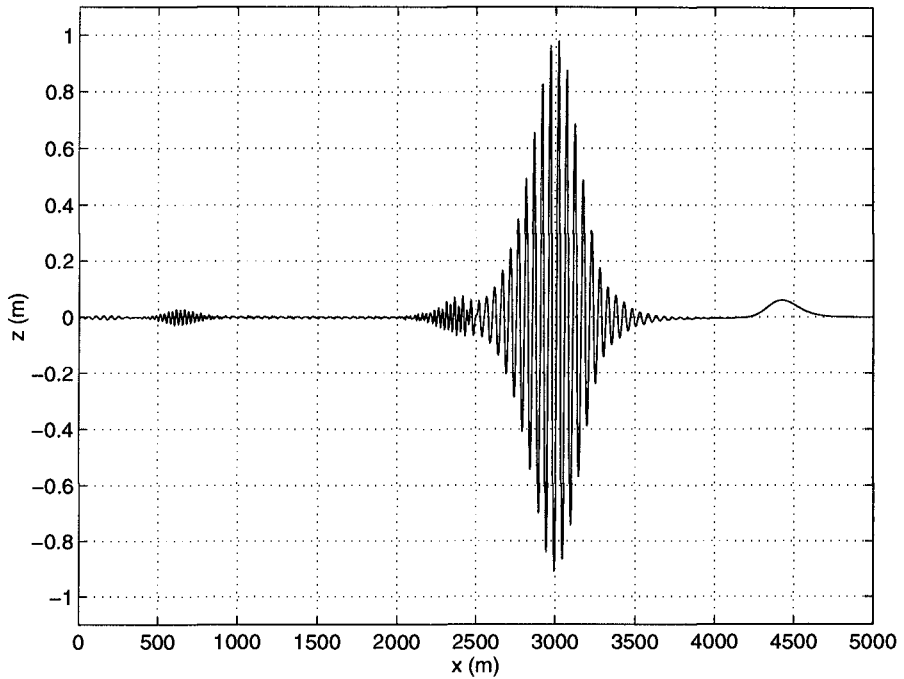


Figure 3: Surface elevation at  $t = 45T$  for run 1

equals 10.85 m/s here. The computations with a contribution of  $\zeta$  and  $\phi_{bl}$  show a reduction of the amplitude of this wave from 6.0 to 2.5 cm.

At the back of the wave group a smaller wave group evolves consisting of carrier waves with wave period approximately 4.2 s. Its amplitude is smallest in run 4 and 6 which contain the second-order contribution  $\eta_2$  and  $\phi_2$ .

In summary it can be said that the differences between the computations presented here can be explained satisfactory by relating them to the contributions to the initial wave signal. However, the second-order contributions in runs 4, 5 and 6 do not prevent the generation of free waves nor do they prevent the generation of a left-going wave signal. At this point it is not clear whether this is due to the imposition of the boundary condition at the actual free surface or to the restriction to only second-order contributions. The use of formula (7) on the second-order part of the wave signal and the use of more higher-order contributions may improve the stationary character of the signal. Nevertheless it is possible to investigate the influence of bottom topography on the generation of free-long waves, but one has to take into account the generation of the spurious waves shown in these computations.

A closer study should also include the effect of the dispersive and dissipative

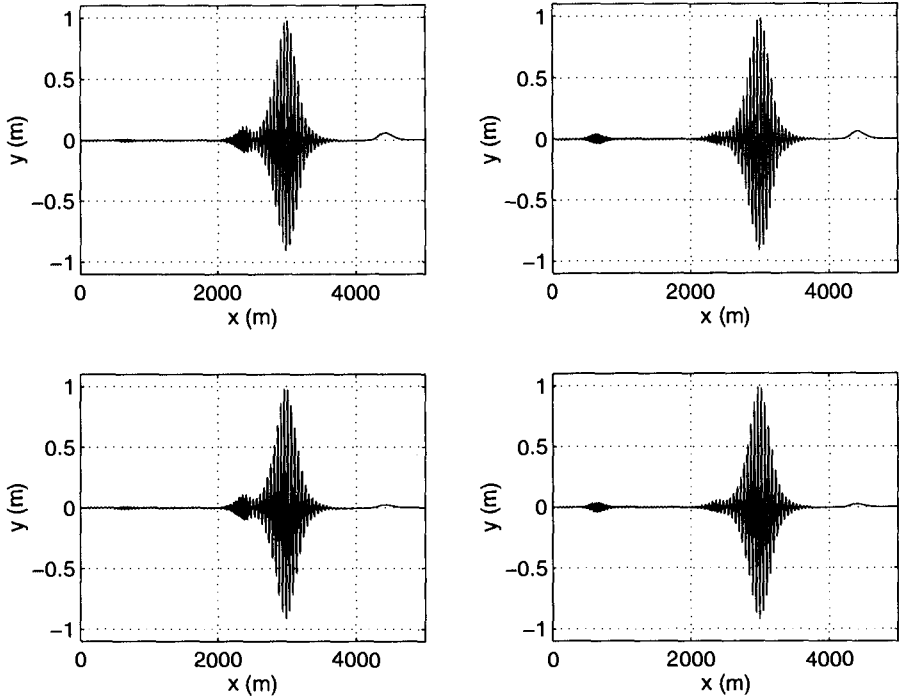


Figure 4: Surface elevation at  $t = 45T$  for: run 2 (upper left), run 4 (upper right), run 5 (down left) and run 6 (down right)

character of the numerical scheme. Although very small for the resolution used, they may become relatively important when smaller contributions to the wave signal are considered.

The simulations over 60 wave periods took about 1.5 hours on a Cray C98 computer at a computational speed of about 125 Mflop/s. The required memory was approximately 56 MByte. The use of a single domain for this simulation would have exceeded the capacity of the Cray computer. Moreover it is questionable whether the system of linear equations in this case is numerically solvable within the required accuracy.

With an eye to larger problems involving a bottom topography it is remarked again that the computational costs per time step depend at most linearly with the size of the computational domain. For comparison with the results of Dingemans et al. [3] on a domain with a length of 15 km, this implies three times as much computational costs per time step. However, a longer simulation time is required for this domain. The computational costs per simulation will then be an additional factor larger than those presented in this paper. Studies including bottom topography will be continued in due time.

## 5 Conclusions

By using a domain decomposition method in a numerical method for nonlinear waves, it is possible to simulate the propagation of wave groups over large simulation times. For the formulation of a stationary propagating wave group it is important to include higher-order contributions. The release of free waves from the wave group can be explained from second-order contributions to the first-order signal. The question remains however, how to impose an initial signal to obtain a propagating wave group of fixed form over a horizontal bottom.

## Acknowledgements

These investigations were supported by the Dutch Technology Foundation (STW). The use of supercomputer facilities was provided by NCF.

## References

- [1] Broeze, J., E.F.G. van Daalen and P.J. Zandbergen, (1993), *Comp. Mech.*, **13**, pp. 12-28.
- [2] De Haas, P.C.A. and P.J. Zandbergen, (to appear), The application of domain decomposition to time-domain computations of nonlinear water waves with a panel method, *J. Comp. Phys.*
- [3] Dingemans, M.W., H.A.H. Petit, Th.J.G.P. Meijer and J.K. Kostense, (1991), Numerical evaluation of the third-order evolution equations for weakly nonlinear water waves propagating over uneven bottoms. In: *Computer Modelling in Ocean Engineering 91*, Barcelona, pp. 361-370.
- [4] Le Tallec, P., (1994), Domain decomposition methods in computational mechanics, *Comp. Mech. Adv.*, **1**, pp. 121-220.
- [5] Liu, P.L-F. and M.W. Dingemans, (1989), Derivation of the third-order evolution equations for weakly nonlinear water waves propagating over uneven bottoms. *Wave Motion*, **11** pp. 41-64.
- [6] Mei, C.C., (1983), The applied dynamics of ocean surface waves, Advanced Series on Ocean Engineering (Vol. 1), World Scientific, Singapore.
- [7] Quarteroni, A., Ed., (1994), *Proc. Sixth Int. Symp. on Domain Decomposition Methods for Partial Differential Equations*, Como, June 1992 (AMS, Providence).
- [8] Wang, P., Y. Yao and M.P. Tulin, (1994), *Int. Journ. of Offshore and Polar Eng.*, **4**, pp. 200-205.